arXiv:1403.2482v1 [cs.CV] 11 Mar 2014

Removing Mixture of Gaussian and Impulse Noise by Patch-Based Weighted Means

Haijuan Hu[a,b], Bing Li[c], Quansheng Liu[b]

[a] *Northeastern University at Qinhuangdao, School of Mathematics and Statistics, Hebei, 066004, China*

[b] *Univ Bretagne-Sud, CNRS UMR 6205, LMBA, Campus de Tohannic, F-56000 Vannes, France*

[c] *Zhongshan Polytechnic, Department of Math., Zhongshan, 528404, China*

Abstract

We first establish a law of large numbers and a convergence theorem in distribution to show the rate of convergence of the non-local means filter for removing Gaussian noise. We then introduce the notion of degree of similarity to measure the role of similarity for the non-local means filter. Based on the convergence theorems, we propose a patch-based weighted means filter for removing impulse noise and its mixture with Gaussian noise by combining the essential idea of the trilateral filter and that of the non-local means filter. Our experiments show that our filter is competitive compared to recently proposed methods.

Keywords: Gaussian noise, Impulse noise, Trilateral filter, Non-local means filter, Convergence theorem, Degree of similarity

1. Introduction

Images are produced to record or display useful information. Due to the visibility of images and the rapid development of science and technology, images play an increasingly important role in our lives. However, because of imperfections in the imaging and capturing process, the recorded image invariably represents a degraded version of the original scene ([2, 4]). The

Email addresses: huhaijuan61@126.com (Haijuan Hu), libcs@263.net (Bing Li), Quansheng.Liu@univ-ubs.fr (Quansheng Liu)

undoing of these imperfections is crucial to many of the subsequent image processing tasks.

There exists a wide range of different degradations. A very important example is the existence of noise. Noise may be introduced by the medium through which the image is created and transmitted. In this paper, we concentrate on removing impulse noise and its mixture with Gaussian noise.

We present a numerical image by a $M \times N$ matrix $u = \{u(i) : i \in I\}$, where $I = \{0, 1, \ldots, M-1\} \times \{0, 1, \ldots, N-1\}$ is the image domain, and $u(i) \in \{0, 1, 2, \ldots, 255\}$ represents the gray value at the pixel i for 8-bit gray images. The additive Gaussian noise model is:

$$v(i) = u(i) + \eta(i),$$

where $u = \{u(i) : i \in I\}$ is the original image, $v = \{v(i) : i \in I\}$ is the noisy one, and η is the Gaussian noise: $\eta(i)$ are independent and identically distributed Gaussian random variables with mean 0 and standard deviation σ. In the sequel we always denote by u the original image, and v the noisy one. The random impulse noise model is:

$$v(i) = \begin{cases} \eta(i) & \text{with probability } p, \\ u(i) & \text{with probability } (1-p), \end{cases}$$

where $0 < p < 1$ is the impulse probability (the proportion of the occurrence of the impulse noise), and $\eta(i)$ are independent random variables uniformly distributed on $[\min\{u(i) : i \in I\}, \max\{u(i) : i \in I\}]$, generally taken as [0,255] for 8-bit gray images. The task of image denoising is to recover the unknown original image u as well as possible from the degraded one v.

There are a lot of denoising methods in the literature. To remove Gaussian noise, there are approaches based on wavelets [14, 9, 6], approaches based on variational models [27, 15], and weighted means approaches [36, 28, 29, 3, 21], etc. A very important progress is the proposition of the non-local means filter (NL-means) [3], which estimates original images by weighted means along similar local patches. Since then, many researchers combined the ideas of "local patch" and other methods to remove noise, for instance [17, 10, 24, 19]. There are also many methods to remove impulse noise including, for example, median based filters [26, 7, 1], fuzzy filters [37], variational based methods [25, 5, 13].

Because Gaussian noise and impulse noise have different characters, the above-mentioned methods can only be used for removing only one kind of

noise (Gaussian noise or impulse noise), and can not be applied to remove a mixture of Gaussian noise and impulse noise. To remove mixed noise, a successful method is the trilateral filter [18]: it introduces an interesting statistic called ROAD (Rank of Ordered Absolute Differences) to detect impulse noisy pixels, and combines it with the bilateral filter [28, 29] to remove noise. The trilateral filter [18] is also effective for removing impulse noise; a variant of the ROAD statistic, named ROLD (Rank-Ordered Logarithmic Difference), has been proposed in [13], where it is combined with the edge-preserving variational method [5] for removing impulse noise. Other methods have also been developed recently to remove mixed noise. The papers [22, 20, 33, 11, 12] use the patch-based idea of NL-means to remove impulse noise and mixed noise. In [22, 20], generalizations of NL-means are proposed for removing impulse noise and its mixture with Gaussian noise with the help of the ROAD statistics [18]; the main idea is to define weights in terms of the ROAD statistics and the similarity of local patches, which are nearly zero for impulse noisy points. In [33], NL-means is adapted by estimating the similarity of patches with the reference image obtained in an impulse noise detection mechanism. The papers [11, 12] also use a patch-based approach: they introduce a robust distance inspired by order statistics to estimate the similarity between patches using the tail of the binomial distribution, and use the maximum likelihood estimator (MLE) to estimate the original image. The methods in [35] and [32, 38] use the ideas of the state-of-the-art Gaussian noise removal methods BM3D [10] and K-SVD [17] respectively to remove mixed noise; the algorithm proposed in [23] is based on a Bayesian classification of the input pixels, which is combined with the kernel regression framework.

The success of NL-means [3] explores in a nice way the similarity phenomenon which is widespread in natural images. Many filters have been developed based on the basic idea of NL-means as stated before. But the theoretic aspects have not been so much studied. A probabilistic explanation called similarity principle is given in [22]. Here we improve this principle by proving a Marcinkiewicz law of large numbers and a convergence theorem in distribution, which describe the rate of convergence of NL-means. We will also introduce the notion of degree of similarity to estimate the influence of similarity on NL-means. Based on the convergence theorems, we propose a new filter, called patch-based weighted means filter (PWMF) to improve the mixed noise filter (MNF) introduced in [22]. Compared to MNF, the new filter simplifies the joint impulse factor in MNF, adds a spatial factor, and adjusts the choice of parameters. Experimental results show that our

new filter is competitive both for removing impulse noise and mixed noise compared to recently developed filters [18, 35, 32, 33, 12]. For the sake of completeness, let us mention that this paper is an extended and improved version of the conference proceeding version [20].

This paper is organized as follows. In Section 2, we recall the non-local means filter [3], establish two convergence theorems to show the rate of convergence of NL-means, and introduce the notion of degree of similarity. In Section 3, we recall the trilateral filter [18] and introduce our new filter. Experiments are presented in Section 4. Conclusions are made in Section 5.

2. Convergence Theorems for Non-Local Means

In this section, we first establish a Marcinkiewicz law of large numbers and a convergence theorem in distribution for NL-means [3]. We then introduce the notion of degree of similarity to measure the role of similarity in image restoration.

2.1. Non-Local Means

For $i \in I$ and d an odd integer, let $\mathcal{N}_i(d) = \{j \in I : |j-i| \leq (d-1)/2\}$ be the window with center i and size $d \times d$, where $|j-i| = \max(|j_1-i_1|, |j_2-i_2|)$ for $i = (i_1, i_2)$ and $j = (j_1, j_2)$. And set $\mathcal{N}_i^0(d) = \mathcal{N}_i(d) \backslash \{i\}$. We sometimes simply write $\mathcal{N}_i$ and $\mathcal{N}_i^0$ for $\mathcal{N}_i(d)$ and $\mathcal{N}_i^0(d)$, respectively. Denote $v(\mathcal{N}_i) = \{v(k) : k \in \mathcal{N}_i\}$ as the vector composed of the gray values of v in the window $\mathcal{N}_i$ arranged lexicographically.

The denoised image by NL-means is given by

$$\mathrm{NLM}(v)(i) = \frac{\sum_{j \in \mathcal{N}_i(D)} w(i,j) v(j)}{\sum_{j \in \mathcal{N}_i(D)} w(i,j)}, \quad i \in I, \tag{1}$$

with

$$w(i,j) = e^{-||v(\mathcal{N}_i) - v(\mathcal{N}_j)||_a^2 / (2\sigma_r^2)}, \tag{2}$$

where $\sigma_r > 0$ is a control parameter,

$$||v(\mathcal{N}_i) - v(\mathcal{N}_j)||_a^2 = \frac{\sum_{k \in \mathcal{N}_i(d)} a(i,k) |v(k) - v(\mathcal{T}(k))|^2}{\sum_{k \in \mathcal{N}_i(d)} a(i,k)}, \tag{3}$$

$a(i,k) > 0$ being some fixed weights usually chosen to be a decreasing function of the Euclidean norm $\|i-k\|$ or $|i-k|$, and $\mathcal{T} = \mathcal{T}_{ij}$ is the translation

mapping of $\mathcal{N}_i$ onto $\mathcal{N}_j$: $\mathcal{T}(k) = k - i + j, k \in \mathcal{N}_i$. Originally, $\mathcal{N}_i(D)$ in (2) is chosen as the whole image I, but in practice, it is better to choose $\mathcal{N}_i(D)$ with an appropriate number D. We call $\mathcal{N}_i(D)$ search windows, and $\mathcal{N}_i = \mathcal{N}_i(d)$ local patches.

2.2. Convergence Theorems

2.2.1. Convergence Theorems for NL-means

We now present two convergence theorems for NL-means using probability theory. For simplicity, we use the same notation $v(\mathcal{N}_i)$ to denote both the observed image patch centered at i and the corresponding random variable (in fact the observed image is just a realization of the corresponding variable). Therefore the distribution of the observed image $v(\mathcal{N}_i)$ is just that of the corresponding random variable.

Definition 1. *Two patches $v(\mathcal{N}_i)$ and $v(\mathcal{N}_j)$ are called similar if they have the same probability distribution.*

Definition 1 is a probabilistic interpretation of the similarity phenomenon. According to this definition, two observed patches $v(\mathcal{N}_i)$ and $v(\mathcal{N}_j)$ are similar if they are issued from the same probability distribution.

The following theorem is a kind of Marcinkiewicz law of large numbers. It gives an estimation of the almost sure convergence rate of the estimator to the original image for the non-local means filter.

Theorem 1. *Let $i \in I$ and let I_i be the set of j such that the patches $v(\mathcal{N}_i)$ and $v(\mathcal{N}_j)$ are similar (in the sense of Definition 1). Set*

$$v^0(i) = \frac{\sum_{j \in I_i} w^0(i,j) v(j)}{\sum_{j \in I_i} w^0(i,j)}, \tag{4}$$

where

$$w^0(i,j) = e^{-\|v(\mathcal{N}_i^0) - v(\mathcal{N}_j^0)\|_a^2 / (2\sigma_r^2)}. \tag{5}$$

Then for any $\epsilon \in (0, \frac{1}{2}]$, as $|I_i| \to \infty$,

$$v^0(i) - u(i) = o(|I_i|^{-(\frac{1}{2} - \epsilon)}) \quad \textit{almost surely}, \tag{6}$$

where $|I_i|$ denotes the cardinality of I_i.

Notice that when $\epsilon = \frac{1}{2}$, (6) means that

$$\lim_{|I_i|\to\infty} v^0(i) = u(i) \quad \text{almost surely,} \tag{7}$$

which is the similarity principle in [22].

Recall that $\mathcal{N}_i^0 = \mathcal{N}_i \backslash i$. Theorem 1 shows that $v^0(i)$ is a good estimator of the original image $u(i)$ if the number of similar patches $|I_i|$ is sufficiently large. Here we use the weight $w^0(i,j)$ instead of $w(i,j)$, as $w^0(i,j)$ has the nice property that it is independent of $v(j)$ if $j \notin \mathcal{N}_i$. This property is used in the proof, and makes the estimator $v^0(i)$ to be "almost" non-biased: in fact, if the family $\{v(j)\}_j$ is independent of the family $\{w^0(i,j)\}_j$ (e.g. this is the case when the similar patches are disjoint), then it is evident that $\mathbb{E}v^0(i) = u(i)$. We can consider that this non-biased property holds approximately as for each j there are few k such that $w^0(i,k)$ is dependent of $v(j)$. A closely related explanation about the biased estimation of NL-means can be found in [34].

Notice that when $v(\mathcal{N}_j)$ is not similar to $v(\mathcal{N}_i)$, the weight $w^0(i,j)$ is small and negligible. Therefore it is also reasonable to take all patches for the calculation. But selecting only similar patches can improve the restoration result, and can also speed up the algorithm. The difference between $w^0(i,j)$ and $w(i,j)$ is also small, so that Theorem 1 shows that $\mathrm{NLM}(v)(i)$ is also a good estimator of $u(i)$. But very often $v^0(i)$ gives better restoration result.

The next result is a convergence theorem in distribution. It states that $v^0(i) - u(i) \to 0$ in distribution with a rate as $1/\sqrt{|I_i|}$.

Theorem 2. *Under the condition of Theorem* 1*, assume additionally that* $\{v(\mathcal{N}_j) : j \in I_i\}$ *is a stationary sequence of random vectors. Then as* $|I_i| \to \infty$*,*

$$\sqrt{|I_i|}(v^0(i) - u(i)) \xrightarrow{d} \mathcal{L},$$

where $\xrightarrow{d}$ *means the convergence in distribution, and* $\mathcal{L}$ *is a mixture of centered Gaussian laws in the sense that it has a density of the form*

$$f(t) = \int_{\mathbb{R}^{|\mathcal{N}_i^0|}} \frac{1}{\sqrt{2\pi}c_x} e^{-\frac{t^2}{2c_x^2}} \mu(dx),$$

μ *being the law of* $v(\mathcal{N}_i^0)$ *and* $c_x > 0$*.*

By Theorems 1 and 2, the larger the value of $|I_i|$, the better the approximation of $v^0(i)$ to $u(i)$, that is to say, the more similar patches, the better restored result. This will be confirmed in Section 2.3 where we shall introduce the notion of degree of similarity for images, showing that the larger the degree of similarity, the better the quality of restoration. The proofs of the theorems will be given in Section 2.2.3.

To prove the two theorems, we will show a Marcinkiewicz law of large numbers (Theorem 3) and a convergence theorem in distribution for random weighted means (Theorem 4), which are more general than Theorems 1 and 2, respectively.

2.2.2. Convergence Theorems for Random Weighted Means

Before stating the theorems, we first recall the notion of l-dependence.

Definition 2. *For an integer $l \geq 0$, a sequence of random variables $X_1, X_2, \ldots$ is called to be l-dependent if each subsequence $X_{k_1}, X_{k_2}, \ldots$ is independent whenever $|k_m - k_n| > l$ for all $m, n \geq 1$. (That is, random variables with distances greater than l are independent of each other.)*

Theorem 3. *Let $\{(a_k, v_k)\}$ be a sequence of l-dependent identically distributed random variables, with $\mathbb{E}|a_1|^p < \infty$ and $\mathbb{E}|a_1 v_1|^p < \infty$ for some $p \in [1, 2)$, and $\mathbb{E}a_1 \neq 0$. Then*

$$\frac{\sum_{k=1}^{n} a_k v_k}{\sum_{k=1}^{n} a_k} - \frac{\mathbb{E}a_1 v_1}{\mathbb{E}a_1} = o(n^{-(1-1/p)}) \quad \textit{almost surely.}$$

We need the following lemma to prove it.

Lemma 1. *[22] If $\{X_n\}$ are l-dependent and identically distributed random variables with $\mathbb{E}X_1 = 0$ and $\mathbb{E}|X_1|^p < \infty$ for some $p \in [1, 2)$, then*

$$\lim_{n\to\infty} \frac{X_1 + \ldots + X_n}{n^{1/p}} = 0 \quad \textit{almost surely.}$$

This lemma is a direct consequence of Marcinkiewicz law of large numbers for independent random variables [8](Page 118), since for all $k \in \{1, \ldots, l +$

$1\}, \{X_{i(l+1)+k} : i \geq 0\}$ is a sequence of i.i.d. random variables, and for each positive integer n, we have

$$X_1 + \ldots + X_n = \sum_{k=1}^{l+1} \sum_{i=0}^{m-1} X_{i(l+1)+k} + \sum_{1 \leq k \leq k_0} X_{m(l+1)+k},$$

where m, k_0 are positive integers with $n = m(l+1) + k_0, 0 \leq k \leq l$.

Proof of Theorem 3. Notice that

$$n\Big(\frac{\sum_{k=1}^n a_k v_k}{\sum_{k=1}^n a_k} - \frac{\mathbb{E}a_1 v_1}{\mathbb{E}a_1}\Big) = \frac{n}{(\sum_{k=1}^n a_k)} \frac{1}{\mathbb{E}a_1} \sum_{k=1}^n a_k z_k,$$

where

$$z_k = v_k \mathbb{E}a_1 - \mathbb{E}a_1 v_1.$$

Since $\mathbb{E}|a_1| \leq (\mathbb{E}|a_1|^p)^{1/p} < \infty$, by Lemma 1 with $p = 1$, we have

$$\lim_{n\to\infty} \frac{\sum_{k=1}^n a_k}{n} = \mathbb{E}a_1 \quad \text{almost surely.}$$

Since $\mathbb{E}a_1 z_1 = 0$, and $\mathbb{E}|a_1 z_1|^p < \infty$, again by Lemma 1, we get

$$\lim_{n\to\infty} \frac{\sum_{k=1}^n a_k z_k}{n^{1/p}} = 0 \quad \text{almost surely.}$$

Thus the conclusion follows. □

Theorem 4. *Let $\{(a_k, v_k)\}$ be a stationary sequence of l-dependent and identically distributed random variables with $\mathbb{E}a_1 \neq 0, \mathbb{E}a_1^2 < \infty$, and $\mathbb{E}(a_1 v_1)^2 < \infty$. Then*

$$\sqrt{n}\Big(\frac{\sum_{k=1}^n a_k v_k}{\sum_{k=1}^n a_k} - \frac{\mathbb{E}a_1 v_1}{\mathbb{E}a_1}\Big) \xrightarrow{d} N(0, c^2),$$

that is,

$$\lim_{n\to\infty} \mathbb{P}\Big\{\frac{\sqrt{n}}{c}\Big(\frac{\sum_{k=1}^n a_k v_k}{\sum_{k=1}^n a_k} - \frac{\mathbb{E}a_1 v_1}{\mathbb{E}a_1}\Big) \leq z\Big\} = \Phi(z), \quad z \in \mathbb{R},$$

where

$$\Phi(z) = \frac{1}{\sqrt{2\pi}} \int_{-\infty}^z e^{-\frac{t^2}{2}} dt,$$

and c is a constant.

We need the following lemma to prove the theorem.

Lemma 2. *[31] Let $\{X_n\}$ be a stationary sequence of l-dependent and identically distributed random variables with $\mathbb{E}X_1 = 0$ and $\mathbb{E}X_1^2 = c^2 < \infty$. Set $S_n = X_1 + \ldots + X_n (n \geq 1)$,*

$$c_1 = c^2 + 2\sum_{k=1}^{l} \mathbb{E}X_1 X_{1+k}, \quad \textit{and} \quad c_2 = 2\sum_{k=1}^{l} k\mathbb{E}X_1 X_{1+k}.$$

Then $var(S_n) = c_1 n - c_2$, and as $n \to \infty$,

$$\frac{S_n}{\sqrt{var(S_n)}} \xrightarrow{d} N(0,1).$$

Proof of Theorem 4. As in the proof of Theorem 3, we have

$$\sqrt{n}\Big(\frac{\sum_{k=1}^n a_k v_k}{\sum_{k=1}^n a_k} - \frac{\mathbb{E}a_1 v_1}{\mathbb{E}a_1}\Big) = \frac{n}{(\sum_{k=1}^n a_k)}\frac{1}{\mathbb{E}a_1}\frac{\sum_{k=1}^n a_k z_k}{\sqrt{n}},$$

where

$$z_k = v_k \mathbb{E}a_1 - \mathbb{E}a_1 v_1.$$

Notice that the l-dependence of $\{(a_k, v_k)\}$ and the stationarity imply those of $\{(a_k, z_k)\}$. Therefore by Lemma 2, we get

$$\frac{\sum_{k=1}^n a_k z_k}{\sqrt{n} c_0} \to N(0,1),$$

where

$$c_0 = \sqrt{\mathbb{E}(a_1 z_1)^2 + 2\lambda}, \quad \text{with } \lambda = \sum_{k=1}^{l} \mathbb{E}a_1 z_1 a_{1+k} z_{1+k}.$$

Since $\mathbb{E}|a_1| \leq (\mathbb{E}|a_1|^p)^{1/p}$, by Lemma 1 with $p = 1$, we obtain

$$\lim_{n\to\infty} \frac{\sum_{k=1}^n a_k}{n} = \mathbb{E}a_1 \quad \text{almost surely.}$$

Thus the conclusion follows with $c = c_0(\mathbb{E}a_1)^2$. □

2.2.3. Proofs of the Convergence Theorems 1 *and* 2

For simplicity, denote by $I_i = \{j_1, j_2, \dots j_n\}$ with $n = |I_i|$ in the following proof. We need to prove, for any $\epsilon \in (0, \frac{1}{2}]$, as $n \to \infty$,

$$\frac{\sum_{k=1}^n w^0(i, j_k) v(j_k)}{\sum_{k=1}^n w^0(i, j_k)} - u(i) = o(n^{-(\frac{1}{2}-\epsilon)}) \quad \text{almost surely,}$$

with

$$w^0(i, j_k) = e^{-\|v(\mathcal{N}_i^0) - v(\mathcal{N}_{j_k}^0)\|^2/(2\sigma_r^2)}.$$

We will apply Theorem 3 to prove it. Note that the sequence $\{w^0(i, j_k), v(j_k)\}$ $(k = 1, 2, \dots, n)$ is not l-dependent, since the central random variable $v(\mathcal{N}_i^0)$ is contained in all the terms. To make use of Theorem 3, we first take a fixed vector to replace the central random variable.

Proof of Theorem 1. Fix $x \in \mathbb{R}^{|\mathcal{N}_i^0|}$. Let

$$a_k = w^0(x, j_k) = e^{-\|x - v(\mathcal{N}_{j_k}^0)\|^2/(2\sigma_r^2)},$$

then a_k and $v(j_k)$ are independent since $j_k \notin \mathcal{N}_{j_k}^0$. So

$$\frac{\mathbb{E} a_k v(j_k)}{\mathbb{E} a_k} = \mathbb{E} v(j_k) = u(j_k) = u(i).$$

When $\mathcal{N}_{j_m}^0$ and $\mathcal{N}_{j_n}^0$ are disjoint, $v(\mathcal{N}_{j_m}^0)$ and $v(\mathcal{N}_{j_n}^0)$ are independent, so are a_{j_m} and a_{j_n}, and so are $(a_{j_m}, v(j_m))$ and $(a_{j_n}, v(j_n))$ since x is fixed. Thus $\{(a_k, v(j_k))\}$ is a sequence of l-dependent identically distributed random vectors for l large enough. Since $v = u + \eta$, with the range of u being bounded and η being Gaussian, we have $\mathbb{E}|v(j_k)|^p < \infty$ for $p \in [1, 2)$. (In fact, it holds for all $p \geq 1$.) Thus $\mathbb{E}|a_k v(j_k)|^p < \infty$, as $a_k \leq 1$.

Applying Theorem 3, for fixed $x = v(\mathcal{N}_i^0) \in \mathbb{R}^{|\mathcal{N}_i^0|}$, we have, for any positive integer k_0,

$$\frac{\sum_{k=k_0}^n w^0(x, j_k) v(j_k)}{\sum_{k=k_0}^n w^0(x, j_k)} - u(i) = o(n^{-(1-1/p)}) \quad \text{almost surely.} \tag{8}$$

Now let k_0 be a positive integer such that $v(\mathcal{N}_i^0)$ is independent of $v(\mathcal{N}_{j_k}^0)$ for all $k \geq k_0$. By Fubini's theorem, we can replace $w^0(x, j_k)$ in (8) by

$$w^0(i, j_k) = e^{-\|v(\mathcal{N}_i^0) - v(\mathcal{N}_{j_k}^0)\|^2/(2\sigma_r^2)}.$$

That is,

$$\frac{\sum_{k=k_0}^{n} w^0(i,j_k)v(j_k)}{\sum_{k=k_0}^{n} w^0(i,j_k)} - u(i) = o(n^{-(1-1/p)}) \quad \text{almost surely.} \tag{9}$$

To prove the theorem, we need to estimate the difference between the left-hand sides of (6) and (9). Let

$$A_0 = \sum_{k=1}^{k_0-1} w^0(i,j_k)v(j_k), \quad A_n = \sum_{k=k_0}^{n} w^0(i,j_k)v(j_k),$$

$$B_0 = \sum_{k=1}^{k_0-1} w^0(i,j_k), \quad B_n = \sum_{k=k_0}^{n} w^0(i,j_k).$$

Then as before, fixing $x \in \mathbb{R}^{|\mathcal{N}_i^0|}$, applying Theorem 3 with $p = 1$ and Fubini's theorem, and replacing x by $v(\mathcal{N}_i^0)$, we obtain

$$\lim_{n\to\infty} \frac{A_n}{n} = \mathbb{E}w^0(i,j_k)v(j_k), \quad \text{and } \lim_{n\to\infty} \frac{B_n}{n} = \mathbb{E}w^0(i,j_k).$$

Using this and the fact that

$$\frac{A_0 + A_n}{B_0 + B_n} - \frac{A_n}{B_n} = \frac{A_0 B_n - A_n B_0}{B_n(B_0 + B_n)},$$

we see that

$$\Big| \frac{\sum_{k=k_0}^{n} w^0(i,j_k)v(j_k)}{\sum_{k=k_0}^{n} w^0(i,j_k)} - \frac{\sum_{k=1}^{n} w^0(i,j_k)v(j_k)}{\sum_{k=1}^{n} w^0(i,j_k)} \Big| = O(\frac{1}{n}) \quad \text{almost surely.} \tag{10}$$

Therefore, (9) implies that

$$\frac{\sum_{k=1}^{n} w^0(i,j_k)v(j_k)}{\sum_{k=1}^{n} w^0(i,j_k)} - u(i) = o(n^{-(1-1/p)}) \quad \text{almost surely.} \tag{11}$$

As (11) holds for any $p \in [1,2)$, we see that (6) holds for all $\epsilon \in (0, \frac{1}{2}]$. □

Proof of Theorem 2. Similarly to the proof of Theorem 1, fix $x \in \mathbb{R}^{|\mathcal{N}_i^0|}$, and set $a_k = w^0(x,j_k) = e^{-\|x - v(\mathcal{N}_{j_k}^0)\|^2/(2\sigma_r^2)}$. Then a_k and $v(j_k)$ are independent, and $\mathbb{E}a_k v(j_k)/\mathbb{E}a_k = \mathbb{E}v(j_k) = u(i)$. For l large enough, $\{(a_k, v(j_k))\}$ is a sequence of l-dependent identically distributed random vectors, and

$\mathbb{E}|a_k v(j_k)|^2 \leq \mathbb{E}|v(j_k)|^2 < \infty$. Hence applying Theorem 4, for fixed $x = v(\mathcal{N}_i^0)$, we get, for any positive integer k_0,

$$Z_n(x) := \sqrt{n}\Big(\frac{\sum_{k=k_0}^n w^0(x, j_k)v(j_k)}{\sum_{k=k_0}^n w^0(x, j_k)} - u(i)\Big) \xrightarrow{d} N(0, c_x^2),$$

where $c_x > 0$ depends on x. This means that for any $t \in \mathbb{R}$,

$$\lim_{n\to\infty} \mathbb{P}(Z_n(x) \leq t) = \int_{-\infty}^t \frac{1}{\sqrt{2\pi}c_x} e^{-\frac{z^2}{2c_x^2}} dz.$$

Let k_0 be the positive integer such that $v(\mathcal{N}_i^0)$ is independent of $v(\mathcal{N}_{j_k}^0)$ for all $k \geq k_0$. Then by Fubini's theorem and Lebesgue's dominated convergence theorem, we have

$$\lim_{n\to\infty} \mathbb{P}\Big(Z_n(v(\mathcal{N}_i^0)) \leq t\Big) = \int_{-\infty}^t f(z)dz,$$

where

$$f(z) = \int_{\mathbb{R}^{|\mathcal{N}_i^0|}} \frac{1}{\sqrt{2\pi}c_x} e^{-\frac{z^2}{2c_x^2}} \mu(dx),$$

with μ being the law of $v(\mathcal{N}_i^0)$. In other words,

$$\sqrt{n}\Big(\frac{\sum_{k=k_0}^n w^0(i, j_k)v(j_k)}{\sum_{k=k_0}^n w^0(i, j_k)} - u(i)\Big) \xrightarrow{d} \mathcal{L},$$

where $\mathcal{L}$ is the law with density f. This together with (10) give the conclusion of Theorem 2.

□

2.3. Degree of Similarity

In this section, we introduce the notion of degree of similarity of images to describe the influence of the number of similar patches on the restoration results.

If two patches $v(\mathcal{N}_i)$ and $v(\mathcal{N}_j)$ have the same distribution and are independent of each other, then $\{v(k) - v(\mathcal{T}(k)) : k \in \mathcal{N}_i\}$ are independent variables with the same law $N(0, 2\sigma^2)$ (recall that $\mathcal{T}$ is the translation mapping of $\mathcal{N}_i$ onto $\mathcal{N}_j$). Therefore

$$\|v(\mathcal{N}_i) - v(\mathcal{N}_j)\|^2 = \sum_{k\in\mathcal{N}_i} |v(k) - v(\mathcal{T}(k))|^2 = 2\sigma^2 X,$$

where X is the sum of squares of independent random variables with normal law $N(0,1)$, and has the law χ^2 with $|\mathcal{N}_i| = d^2$ degrees of liberty. For $\alpha \in (0,1)$, let $T_\alpha > 0$ be determined by

$$\mathbb{P}(X > \frac{T_\alpha^2}{2\sigma^2}) = \alpha,$$

so that

$$\mathbb{P}(\|v(\mathcal{N}_i) - v(\mathcal{N}_j)\| \leq T_\alpha) = 1 - \alpha.$$

The value of α is chosen to be small enough. It represents the risk probability. When $\mathbb{P}(\|v(\mathcal{N}_i) - v(\mathcal{N}_j)\| \leq T_\alpha$, we consider that $v(\mathcal{N}_i)$ and $v(\mathcal{N}_j)$ are similar with confidence level $1 - \alpha$. This leads us to the following definition of the degree of similarity.

Definition 3. *For $i \in I$, let*

$$DS_i = \frac{\#\{j \in \mathcal{N}_i(D) : \|v(\mathcal{N}_i) - v(\mathcal{N}_j)\| \leq T_\alpha\}}{D^2}$$

be the proportion of patches $v(\mathcal{N}_j)$ similar to $v(\mathcal{N}_i)$ in the search window $\mathcal{N}_i(D)$, and let

$$DS = \frac{\sum_{i \in I} DS_i}{MN}$$

be their mean over the whole image. Define DS the degree of similarity of the image v with confidence level $1 - \alpha$.

We compute the DS values for different images corrupted by Gaussian noise with $\sigma = 10, 20, 30$. Note that the DS values depend on α, d, D, σ. In our experiments, we fix $\alpha = 0.1$. The DS values of noisy images are shown in Table 1. It can be seen that, for non-local means based methods, for example, our method in Section 3.2, generally, the larger the DS value, the larger the PSNR value (see Section 4.2).

3. Patch-Based Weighted Means Filter

In this section, we introduce our new filter which combines the basic idea of NL-means [3] and that of the trilateral filter [18].

Table 1: DS values of noisy images ($\alpha = 0.1, d = 9$)

σ	T_α	D	Lena	Bridge	Peppers256	Peppers512	Boats
10	111.39	7	0.42	0.06	0.29	0.39	0.25
20	279.54	11	0.54	0.15	0.39	0.54	0.40
30	589.33	15	0.55	0.18	0.38	0.55	0.42

3.1. Trilateral Filter

The authors of [18] proposed a neighborhood filter called the trilateral filter as an extension of the bilateral filter [28, 29] to remove random impulse noise and its mixture with Gaussian noise. Firstly, they introduced the statistic ROAD (Rank of Ordered Absolute Differences) to measure how like a point is an impulse noisy point defined by

$$\mathrm{ROAD}(i) = r_1(i) + \cdots + r_m(i), \tag{12}$$

$r_k(i)$ being the k-th smallest term in the set $\{|u(i) - u(j)| : j \in \mathcal{N}_i(d)\backslash\{i\}\}$, d and m two constants taken as $d = 1, m = 4$ in [18]. If i is an impulse noisy point, then $\mathrm{ROAD}(i)$ is large; otherwise it is small. Therefore, the ROAD statistic serves to detect impulse noisy points.

Secondly, with the ROAD statistic, they defined the impulse factor $w_I(i)$ and the joint impulse factor $J_I(i, j)$:

$$w_I(i) = e^{-\frac{\mathrm{ROAD}(i)^2}{2\sigma_I^2}}, \tag{13}$$

$$J_I(i,j) = e^{-\left(\frac{\left(\mathrm{ROAD}(i)+\mathrm{ROAD}(j)\right)}{2}\right)^2 / (2\sigma_J^2)}, \tag{14}$$

where σ_I and σ_J are control parameters[1]. If i is an impulse noisy point, then the value of $w_I(i)$ is close to 0; otherwise it is close to 1. Similarly, if either i or j is an impulse noisy point, then the value of $J_I(i, j)$ is close to 0; otherwise it is close to 1.

Finally, the restored image by the trilateral filter is

$$\mathrm{TriF}(v)(i) = \frac{\sum_{j\in\mathcal{N}_i(D)} w(i,j)v(j)}{\sum_{j\in\mathcal{N}_i(D)} w(i,j)}, \tag{15}$$

[1]In fact, [18] defines the joint impulse factor as $J(i, j) = 1 - J_I(i, j)$. However, it seems to be more convenient to use $J_I(i, j)$ than $J(i, j)$ [22].

where

$$w(i,j) = w_S(i,j) w_R(i,j)^{J_I(i,j)} w_I(j)^{1-J_I(i,j)},$$

with

$$w_S(i,j) = e^{-\frac{|i-j|^2}{2\sigma_S^2}}, \quad w_R(i,j) = e^{-\frac{(v(i)-v(j))^2}{2\sigma_R^2}}.$$

3.2. Patch-Based Weighted Means Filter

As in the non-local means filter [3], our filter estimates each point by the weighed means of its neighbors, and the weight for each neighbor is determined by the similarity of local patches centered at the estimated point and the neighbor. Due to the existence of impulse noise, some points are totally destroyed, so that noisy values are not related to original values at all. So we have to diminish the influence of impulse noisy points. Similarly to [22, 20], we introduce the following weighted norm:

$$||v(\mathcal{N}_i) - v(\mathcal{N}_j)||_M^2 = \frac{\sum_{k \in \mathcal{N}_i^0} w_{S,M}(i,k) F(k, \mathcal{T}(k)) \left|v(k) - v(\mathcal{T}(k))\right|^2}{\sum_{k \in \mathcal{N}_i^0} w_{S,M}(i,k) F(k, \mathcal{T}(k))}, \tag{16}$$

where

$$w_{S,M}(i,k) = e^{-\frac{|i-k|^2}{2\sigma_{S,M}^2}}, \quad F(k, \mathcal{T}(k)) = w_I(k) w_I(\mathcal{T}(k)). \tag{17}$$

Recall that here $k = (k_1, k_2)$ represents a two-dimensional spatial location of a pixel, w_I is defined in (13), and $\mathcal{T}$ is the translation mapping of $\mathcal{N}_i(d)$ onto $\mathcal{N}_j(d)$. $F(k, \mathcal{T}(k))$ is a joint impulse factor: if k or $\mathcal{T}(k)$ is an impulse noisy point, then $F(k, \mathcal{T}(k))$ is close to 0, so that these points contribute little to the weighted norm; otherwise $F(k, \mathcal{T}(k))$ is close to 1.

We now define our filter that we call *Patch-based Weighted Means Filter* (PWMF). The restored image by PWMF is defined as

$$\mathrm{PWMF}(v)(i) = \frac{\sum_{j \in \mathcal{N}_i(D)} w(i,j) v(j)}{\sum_{j \in \mathcal{N}_i(D)} w(i,j)}, \tag{18}$$

where

$$w(i,j) = w_S(i,j) w_I(j) w_M(i,j),$$

with

$$w_S(i,j) = e^{-|i-j|^2/(2\sigma_S^2)}, \quad w_M(i,j) = e^{-||v(\mathcal{N}_i)-v(\mathcal{N}_j)||_M^2/(2\sigma_M^2)}, \tag{19}$$

and $w_I(j)$ is defined in (13). By definition, for each impulse noisy point j in $\mathcal{N}_i(D)$, $w(i,j)$ is close to 0. Hence our new filter can be regarded as an application of the mathematical justifications of the non-local means filter stated in Section 2 to the remained image (which can be considered to contain only Gaussian noise) obtained after filtering the impulse noisy points by the weighted norm (16).

Finally, we mention that, in this paper, we use the joint impulse factor $F(k, \mathcal{T}(k)) = w_I(k)w_I(\mathcal{T}(k))$, which is different from the choice in [22] and [20], where $F(k, \mathcal{T}(k)) = J_I(k, \mathcal{T}(k))$. In fact, we can see that with this new choice, we simplify the methods in [22] and [20] by eliminating a parameter and speeding up the implementation. Furthermore, we empirically find that the new choice leads to an improvement of the quality of restored images, especially for impulse noise.

4. Simulations

4.1. Choices of Parameters

Notice that PWMF reduces to NL-means when $\sigma_I = \sigma_S = \infty$. So for removing Gaussian noise, a reasonable choice is to take σ_I and σ_S large enough. Now we present the choices of parameters for removing impulse noise and mixed noise, which are important for our filter.

In the calculation of ROAD (cf.(12)), we choose 3×3 neighborhoods and $m = 4$. For impulse noise or mixed noise with $p = 0.4, 0.5$, to further improve the results, 5×5 neighborhoods and $m = 12$ are used to calculate ROAD. Now we come to the choice of σ_I, σ_M, σ_S, $\sigma_{S,M}$ appearing in (13), (19) and (17). To remove impulse noise, we use $\sigma_M = 3 + 20p$, $\sigma_S = 0.6 + p$, and omit the factor $w_{S,M}$ (i.e. $\sigma_{S,M}$ can be taken a value large enough); $\sigma_I = 50$ for $p = 0.2, 0.3$, and $\sigma_I = 160$ for $p = 0.4, 0.5$. For mixed noise, we use $\sigma_I = 50 + 5\sigma/3$, $\sigma_M = 3 + 0.4\sigma + 20p$, $\sigma_{S,M} = 2$, and omit the factor w_S. The patch size $d = 9$ is used in all cases; the search window sizes D are shown in Table 2. For other values of σ or p, we choose parameters by linear interpolation or according to the adjacent values of σ or p. It is not easy to find appropriate parameters for a filter. Different choices of parameters can have great influence to the restored images. See also [12]. Some similar

Table 2: Choice of search window sizes D for PWMF

	$\sigma = 0$	$\sigma = 10$	$\sigma = 20$	$\sigma = 30$
D	7	7	11	15

research for NL-means can be found in [34, 30, 16]. Note that our choice of parameters is different from [22]: for the patch size, we use $d = 9$, while [22] uses $d = 3$ in most cases; for impulse noise with $p = 0.4, 0.5$, we use 5×5 neighborhoods for ROAD, while [22] always uses 3×3 neighborhoods.

4.2. Experiments and Comparisons

We use standard gray images to test the performance of our filter[2]. Original images are shown in Fig. 1.[3] As usual we use PSNR (Peak Signal-to-Noise Ratio)

$$\text{PSNR } (\bar{v}) = 10 \log_{10} \frac{255^2 |I|}{\sum_{i \in I} (\bar{v}(i) - u(i))^2} \text{dB}$$

to measure the quality of a restored image, where u is the original image, and $\bar{v}$ the restored one. For the simulations, the gray value of impulse noise is uniformly distributed on the interval [0,255]. We add Gaussian noise and then add impulse noise for the simulation of mixed noise. We use same realizations of noisy images for comparisons of different methods when codes are available, that is, for TriF [18], ROLD-EPR [13], NLMixF [20] and MNF [22]. For other methods, we list the reported results in papers.

The results for TriF are obtained by the program made by ourselves. To compare the performance of our filter with those of TriF fairly, we make our effort to obtain the best results as we can according to the suggestion of [18]. We use $\sigma_I = 40, \sigma_J = 50, \sigma_S = 0.5$, and $\sigma_R = 2\sigma_{QGN}$, where σ_{QGN} is an estimator for the standard deviation of "quasi-Gaussian" noise defined in [18]. For impulse noise, we apply one iteration for $p = 0.2$, two iterations for $p = 0.3, 0.4$, and four iterations for $p = 0.5$. For mixed noise, we apply TriF

[2]The code of our method and the images can be downloaded at https://www.dropbox.com/s/oylg9to8n6029hh/to_j_sci_comput_paper_code.zip.

[3] The images Lena, Peppers256 and Boats are originally downloaded from http://decsai.ugr.es/∼javier/denoise/test_images/index.htm;
the image Peppers512 is from http://perso.telecom-paristech.fr/∼delon/Demos/Impulse and the image Bridge is from www.math.cuhk.edu.hk/∼rchan/paper/dcx/.

twice with different values of σ_S as suggested in [18]: with all impulse noise levels p, for $\sigma = 10$, we first use $\sigma_S = 0.3$, then $\sigma_S = 1$; for $\sigma = 20$, first $\sigma_S = 0.3$, then $\sigma_S = 15$; for $\sigma = 30$, first $\sigma_S = 15$, then $\sigma_S = 15$.

For ROLD-EPR, the listed values are the best PSNR values along iterations with the code from the authors of [13].

Table 3 shows the performances of PWMF for removing impulse noise by comparing with TriF [18], ROLD-EPR [13], PARIGI [12], and NLMixF [20]. For ease of comparison, in this and following tables, we show in bold the best results and the results where the differences from the best ones are less than 0.1dB. We can see that our filter PWMF attains the best performance in term of PSNR. Some visual comparisons are shown in Figs 2 and 3. Carefully comparing these images, we observe that TriF loses some small textured details, while ROLD-EPR is not smooth enough. PARIGI and PWMF show better results.

Different papers consider different mixtures of Gaussian noise and impulse noise. We show the performance of PWMF for removing mixed noise in Tables 4, 5, 6, and 7 by comparing it with TriF [18], NLMixF [20], PARIGI [12] IPAMF+BM [35], Xiao [32], MNF [22], and Zhou [38]. All these comparisons show good performance of our filter except for Barbara when comparing with PARIGI. Our method does not work very well as PARIGI for Barbara, because the ROAD statistics is a very local statistics and can not use the redundancy of this image very well to detect impulse noisy pixels, while PARIGI is particularly powerful for the restoration of textured regions. From Fig. 4, we can see that the results of our filter are visually better than TriF. From Fig. 5, we can see that when the standard deviation σ is high, our filter is smoother than PARIGI, while PARIGI seems to preserve more weak textured details, but it has evident artifacts throughout the whole image (see the electronic version of this paper at full resolution).

Finally, we compare the CPU time of TriF [18], NLMixF [20], and our method PWMF for removing mixed nose in seconds in the platform of MATLAB R2011a with unoptimized mex files. The computer is equipped with 2.13GHZ Intel (R) Core (TM) i3 CPU and 3.0 GB memory. The results are presented in Table 8, which demonstrate that PWMF is rather fast: much faster than NLMixF and even faster than TriF when the noise level is low, thanks to the simplified joint impulse factor $F(k, \mathcal{T}(k))$ defined in (17). The results also show that our method is faster than Zhou [38].

Figure 1: Original 512×512 images of Lena, Bridge, Peppers512, Boats. Since in the original Peppers images, there are black boundaries of width of one pixel in the left and top which can be considered as impulse noise, to make an impartial comparison, we compute PSNR for Peppers images after removing all the four boundaries, that is with images of size 510×510 for Peppers512 and 254×254 for Peppers256

Table 3: PSNR values (dB) to remove impulse noise for TriF [18], ROLD-EPR [13], PARIGI [12], NLMixF [20] and our filter PWMF

Lena	$p = 0.2$	$p = 0.3$	$p = 0.4$	$p = 0.5$
TriF	34.75	32.54	31.28	29.37
ROLD-EPR	34.87	32.08	30.81	29.51
PARIGI	35.45	-	31.75	-
NLMixF	35.69	33.13	31.69	29.87
PWMF	**35.90**	**33.45**	**31.98**	**30.17**

Bridge	$p = 0.2$	$p = 0.3$	$p = 0.4$	$p = 0.5$
TriF	26.81	25.25	24.41	23.35
ROLD-EPR	27.60	25.58	24.42	23.45
PARIGI	27.68	-	**24.80**	-
NLMixF	27.77	25.54	24.45	23.33
PWMF	**28.10**	**26.11**	**24.74**	**23.64**

Peppers256	$p = 0.2$	$p = 0.3$	$p = 0.4$	$p = 0.5$
TriF	30.55	28.81	27.67	25.98
ROLD-EPR	31.03	28.10	27.34	25.96
PARIGI	-	-	-	-
NLMixF	31.78	29.38	28.10	26.47
PWMF	**31.93**	**29.64**	**28.34**	**26.78**

Peppers512	$p = 0.2$	$p = 0.3$	$p = 0.4$	$p = 0.5$
TriF	34.52	31.93	31.27	29.76
ROLD-EPR	34.46	32.31	31.12	30.03
PARIGI	34.75	-	31.63	-
NLMixF	34.77	**32.56**	31.73	30.23
PWMF	**35.08**	**32.59**	**31.95**	**30.38**

Boats	$p = 0.2$	$p = 0.3$	$p = 0.4$	$p = 0.5$
TriF	30.22	28.55	27.52	26.10
ROLD-EPR	30.75	28.19	26.95	25.91
PARIGI	31.21	-	27.56	-
NLMixF	31.32	29.01	27.42	26.10
PWMF	**31.83**	**29.58**	**27.67**	**26.48**

Original | Noisy $p = 0.2$ | TriF PSNR = 34.75

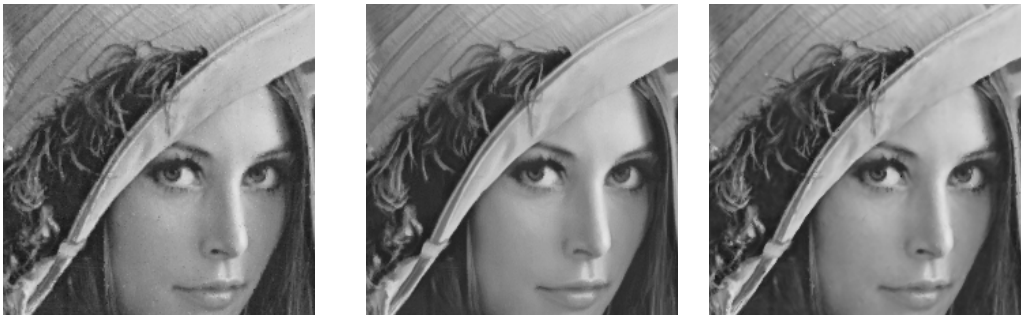

ROLD-EPR PSNR = 34.87 | PARIGI PSNR = 35.45 | PWMF PSNR = 35.90

Figure 2: Comparison of the performances of TriF [18], ROLD-EPR [13], PARIGI [12] and our filter PWMF for removing impulse noise with $p = 0.2$ for Lena

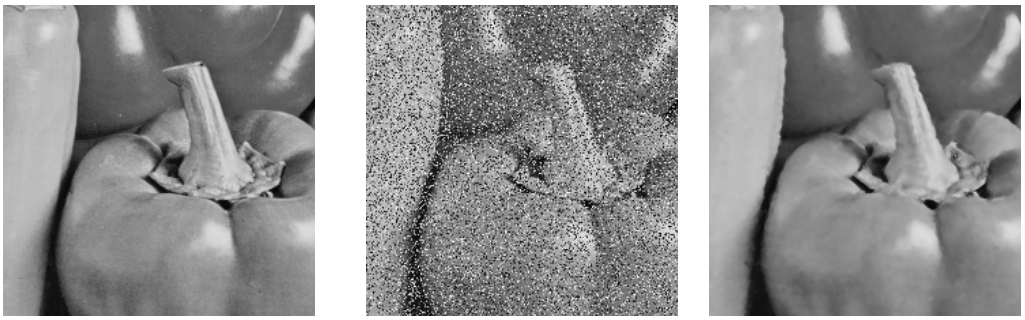

Original | Noisy $p = 0.4$ | TriF PSNR = 31.27

ROLD-EPR PSNR = 31.12 | PARIGI PSNR = 31.63 | PWMF PSNR = 31.95

Figure 3: Comparison of the performances of TriF [18], ROLD-EPR [13], PARIGI [12] and our filter PWMF for removing impulse noise with $p = 0.4$ for Peppers512

Table 4: PSNR values (dB) to remove mixed noise for TriF [18], NLMixF [20] and our filter PWMF. P256 and P512 represent Peppers256 and Peppers512 respectively. For each PSNR value, the corresponding level of Gaussian noise and impulse noise are shown in the top and left of the table

p	$\sigma = 10$			$\sigma = 20$			$\sigma = 30$		
Lena	TriF	NLMixF	PWMF	TriF	NLMixF	PWMF	TriF	NLMixF	PWMF
0.2	31.70	**32.85**	**32.93**	28.75	**30.51**	**30.47**	26.54	**28.70**	**28.67**
0.3	30.77	**31.28**	**31.30**	28.01	**29.41**	**29.38**	25.82	**27.68**	**27.65**
Bridge	TriF	NLMixF	PWMF	TriF	NLMixF	PWMF	TriF	NLMixF	PWMF
0.2	25.28	26.14	**26.35**	23.84	**24.48**	**24.53**	22.50	**23.33**	**23.35**
0.3	24.66	24.73	**25.00**	23.34	23.59	**23.70**	22.08	**22.66**	**22.72**
P256	TriF	NLMixF	PWMF	TriF	NLMixF	PWMF	TriF	NLMixF	PWMF
0.2	29.09	**30.57**	**30.65**	26.82	**28.56**	**28.53**	24.70	**26.73**	**26.71**
0.3	27.89	**28.68**	**28.73**	26.01	**27.16**	**27.13**	23.97	**25.55**	**25.57**
P512	TriF	NLMixF	PWMF	TriF	NLMixF	PWMF	TriF	NLMixF	PWMF
0.2	31.84	**32.64**	**32.70**	29.01	**30.74**	**30.69**	26.82	**29.04**	**29.07**
0.3	30.92	**31.06**	30.93	28.27	**29.55**	29.39	26.01	**27.92**	**27.86**
Boats	TriF	NLMixF	PWMF	TriF	NLMixF	PWMF	TriF	NLMixF	PWMF
0.2	28.37	29.75	**29.91**	26.40	**27.71**	**27.74**	24.58	**26.23**	**26.23**
0.3	27.63	28.15	**28.38**	25.84	**26.66**	**26.75**	24.09	**25.44**	**25.48**

Table 5: PSNR values (dB) to remove mixed noise for PARIGI [12] and our filter PWMF

$p = 0.1\ \sigma = 5$	Lena	Barbara	Cameraman	Boat
PARIGI	34.72	**31.55**	34.98	31.41
PWMF	**35.80**	30.86	**35.80**	**32.60**

$p = 0.3\ \sigma = 15$	Lena	Barbara	Cameraman	Boat
PARIGI	29.22	**27.33**	28.59	26.57
PWMF	**30.25**	25.58	**30.27**	**27.45**

Table 6: PSNR values (dB) for mixed noise removal with (Xiao) [32], (IPAMF+BM) [35], (Zhou) [38] and our filter PWMF

Lena $\sigma = 10$	$p = 0.1$	$p = 0.2$	$p = 0.3$
Xiao	32.75	31.66	30.42
IPAMF+BM	33.61	32.12	30.69
Zhou	**34.25**	32.68	**31.21**
PWMF	34.10	**32.93**	**31.30**

Table 7: PSNR values (dB) for mixed noise removal with MNF [22] and our filter PWMF

Lena	$\sigma = 10, p = 0.2$	$\sigma = 20, p = 0.2$	$\sigma = 30, p = 0.2$
MNF	31.63	29.33	28.40
PWMF	**32.93**	**30.47**	**28.67**

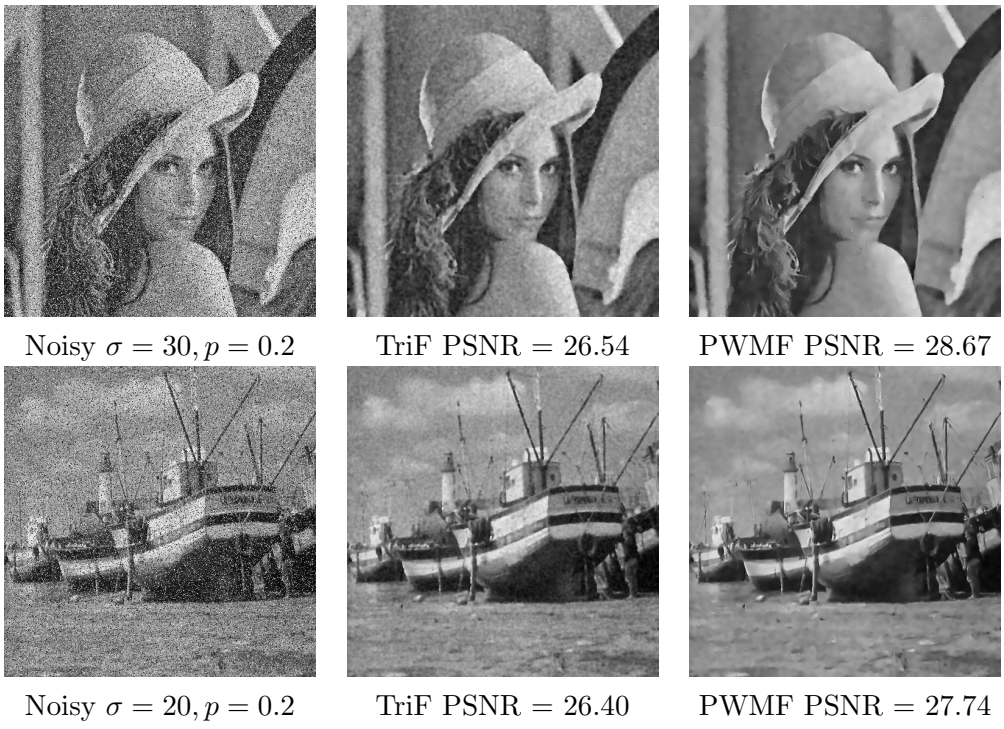

Noisy $\sigma = 30, p = 0.2$ | TriF PSNR = 26.54 | PWMF PSNR = 28.67

Noisy $\sigma = 20, p = 0.2$ | TriF PSNR = 26.40 | PWMF PSNR = 27.74

Figure 4: Comparison of the performances of TriF [18] and our filter PWMF for removing mixed noise

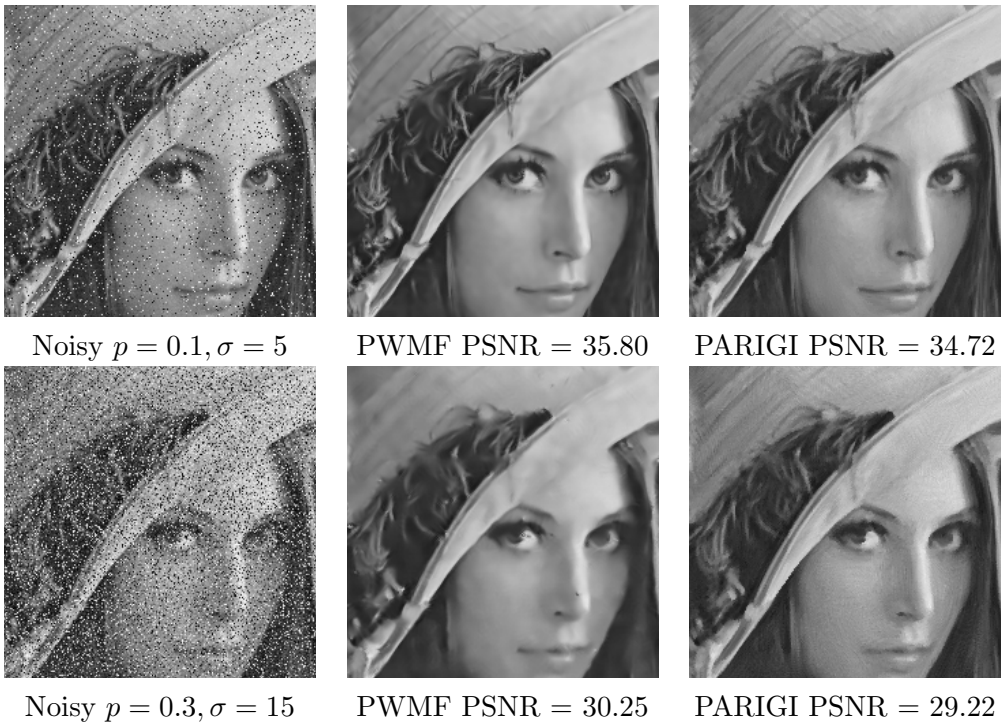

Noisy $p = 0.1, \sigma = 5$ PWMF PSNR = 35.80 PARIGI PSNR = 34.72

Noisy $p = 0.3, \sigma = 15$ PWMF PSNR = 30.25 PARIGI PSNR = 29.22

Figure 5: Comparison of the performances of our filter PWMF and PARIGI [12] for removing mixed noise with Lena

Table 8: Time(s) for TriF [18], NLMixF [20], and PWMF

Image	Noise levels	TriF	NLMixF	PWMF
Lena	$\sigma = 10, p = 0.2$	6.9	60.6	5.4
Lena	$\sigma = 20, p = 0.3$	7.9	170.0	16.7

5. Conclusions and Further Work

Two convergence theorems, one for the almost sure convergence and the other for the convergence in law, are established to show the rate of convergence of NL-means [3]. The notion of degree of similarity is also introduced to describe the influence of the proportion of similar patches in the application of NL-means. Based on the convergence theorems, a new filter called patch-based weighted means filter (PWMF) is proposed to remove mixed noise, leading to an extension of NL-means. The choice of parameters has been carefully discussed. Simulation results show that the new proposed filter is competitive compared to recently developed known algorithms.

As the detection of impulse noise is crucial for removing the noise, which is done by the statistics ROAD [18] in this paper, we could further improve our results by improving ROAD. In the future, we will consider a semi-local statistics to make use of redundancies of images, which has the possibility to well recover the textured regions.

References

[1] Akkoul, S., Ledee, R., Leconge, R., Harba, R.: A new adaptive switching median filter. Signal processing letters, IEEE **17**(6), 587–590 (2010)

[2] Bovik, A.: Handbook of image and video processing. Academic Press (2005)

[3] Buades, A., Coll, B., Morel, J.: A review of image denoising algorithms, with a new one. Multiscale Model. Simul. **4**(2), 490–530 (2005)

[4] Castleman, K.: Digital image processing. Prentice Hall Press, Upper Saddle River, NJ (1996)

[5] Chan, R., Hu, C., Nikolova, M.: An iterative procedure for removing random-valued impulse noise. Signal Processing Letters, IEEE **11**(12), 921–924 (2004)

[6] Chang, S.G., Yu, B., Vetterli, M.: Adaptive wavelet thresholding for image denoising and compression. IEEE Trans. Image Process. **9**, 1532–1546 (2000)

[7] Chen, T., Wu, H.: Adaptive impulse detection using center-weighted median filters. Signal Processing Letters, IEEE **8**(1), 1–3 (2001)

[8] Chow, Y., Teicher, H.: Probability theory: independence, interchangeability, martingales. Springer Verlag (2003)

[9] Coifman, R., Donoho, D.: Translation-invariant denoising. Wavelets and statistics **103**, 125–150 (1995)

[10] Dabov, K., Foi, A., Katkovnik, V., Egiazarian, K.: Image denoising by sparse 3-D transform-domain collaborative filtering. IEEE Trans. Image Process. **16**(8), 2080–2095 (2007)

[11] Delon, J., Desolneux, A.: A patch-based approach for random-valued impulse noise removal. In: 2012 IEEE International Conference on Acoustics, Speech and Signal Processing (ICASSP), pp. 1093–1096. IEEE (2012)

[12] Delon, J., Desolneux, A.: A patch-based approach for removing impulse or mixed gaussian-impulse noise. SIAM Journal on Imaging Sciences **6**(2), 1140–1174 (2013)

[13] Dong, Y., Chan, R., Xu, S.: A detection statistic for random-valued impulse noise. IEEE Trans. Image Process., **16**(4), 1112–1120 (2007)

[14] Donoho, D., Johnstone, J.: Ideal spatial adaptation by wavelet shrinkage. Biometrika **81**(3), 425–455 (1994)

[15] Durand, S., Froment, J.: Reconstruction of wavelet coefficients using total variation minimization. SIAM Journal on Scientific computing **24**(5), 1754–1767 (2003)

[16] Duval, V., Aujol, J., Gousseau, Y.: A bias-variance approach for the nonlocal means. SIAM J. Imaging Sciences **4**, 760–788 (2011)

[17] Elad, M., Aharon, M.: Image denoising via sparse and redundant representations over learned dictionaries. IEEE Trans. Image Process. **15**(12), 3736–3745 (2006)

[18] Garnett, R., Huegerich, T., Chui, C., He, W.: A universal noise removal algorithm with an impulse detector. IEEE Trans. Image Process. **14**(11), 1747–1754 (2005)

[19] Hu, H., Froment, J.: Nonlocal total variation for image denoising. In: Symposium on Photonics and Optoelectronics (SOPO), 2012, pp. 1–4. IEEE (2012)

[20] Hu, H., Li, B., Liu, Q.: Non-local filter for removing a mixture of gaussian and impulse noises. In: G. Csurka, J. Braz (eds.) VISAPP (1), pp. 145–150. SciTePress (2012)

[21] Kervrann, C., Boulanger, J.: Local adaptivity to variable smoothness for exemplar-based image regularization and representation. Int. J. Com. Vis. **79**(1), 45–69 (2008)

[22] Li, B., Liu, Q., Xu, J., Luo, X.: A new method for removing mixed noises. SCIENCE CHINA Information Sciences **54**, 51–59 (2011)

[23] López-Rubio, E.: Restoration of images corrupted by gaussian and uniform impulsive noise. Pattern Recognition **43**(5), 1835–1846 (2010)

[24] Mairal, J., Sapiro, G., Elad, M.: Learning multiscale sparse representations for image and video restoration. Multiscale Modeling & Simulation **7**, 214–241 (2008)

[25] Nikolova, M.: A variational approach to remove outliers and impulse noise. J. Math. Imag. Vis. **20**(1), 99–120 (2004)

[26] Pratt, W.: Median filtering. Semiannual Report, Image Proc. Institute, University of Southern California, Los Angeles, Tech. Rep pp. 116–123 (1975)

[27] Rudin, L.I., Osher, S., Fatemi, E.: Nonlinear total variation based noise removal algorithms. Physica D: Nonlinear Phenomena **60**(1-4), 259–268 (1992)

[28] Smith, S., Brady, J.: SUSAN A new approach to low level image processing. Int. J. Com. Vis. **23**(1), 45–78 (1997)

[29] Tomasi, C., Manduchi, R.: Bilateral filtering for gray and color images. In: Proceedings of the international confernce on computer vision, pp. 839–846. IEEE (1998)

[30] Van De Ville, D., Kocher, M.: Sure-based non-local means. Signal Processing Letters, IEEE **16**(11), 973–976 (2009)

[31] Wen, Z.Y.: Sur quelques théorèmes de convergence du processus de naissance avec interaction des voisins. Bull.Soc.math.France **114**, 403–429 (1986)

[32] Xiao, Y., Zeng, T., Yu, J., Ng, M.: Restoration of images corrupted by mixed gaussian-impulse noise via l sub (1-l) sub (0) minimization. Pattern Recognition **44**(8), 1708–1720 (2011)

[33] Xiong, B., Yin, Z.: A universal denoising framework with a new impulse detector and nonlocal means. IEEE Transactions on Image Processing **21**(4), 1663–1675 (2012)

[34] Xu, H., Xu, J., Wu, F.: On the biased estimation of nonlocal means filter. In: International Conference on Multimedia Computing and Systems/International Conference on Multimedia and Expo, pp. 1149–1152 (2008)

[35] Yang, J.X., Wu, H.R.: Mixed gaussian and uniform impulse noise analysis using robust estimation for digital images. Proceedings of the 16th International Conference on Digital Signal Processing pp. 468–472 (2009)

[36] Yaroslavsky, L.P.: Digital Picture Processing. Springer-Verlag New York, Inc., Secaucus, NJ, USA (1985)

[37] Yuksel, M.: A hybrid neuro-fuzzy filter for edge preserving restoration of images corrupted by impulse noise. IEEE Trans. Image Process., **15**(4), 928–936 (2006)

[38] Zhou, Y., Ye, Z., Xiao, Y.: A restoration algorithm for images contaminated by mixed gaussian plus random-valued impulse noise. Journal of Visual Communication and Image Representation (2013)